

**Ding Chen^{1,*}, Liang Yao¹, Zhenhua Chen^{1,2}, Huiping Wang^{2,3},
Wen Peng^{2,3}**

¹College of Materials Science and Engineering, Hunan University,
Changsha, China

²State Key Laboratory of Cemented carbide, Zhuzhou, China

³ZhuZhou Cemented Carbide Group Co., LTD, Zhuzhou, China

**chendding@hnu.edu.cn*

Investigation on the static fatigue mechanism and effect of specimen thickness on the static fatigue lifetime in WC–Co cemented carbides

The static fatigue mechanism and effect of specimen thickness on static fatigue lifetime for four WC–Co cemented carbides were studied with different binder contents and carbide grain sizes. Static fatigue tests under three-point bend loading were conducted on different sized specimens. The fracture surfaces of rupture specimens were examined by scanning electron microscopy to investigate the static fatigue micromechanisms. Experimental results show that microcracks nucleate from defects or inhomogeneities and the connection of microcracks produces a main crack. The main crack propagates rapidly, resulting in the fracture of specimens. The extension of static fatigue lifetime with the increase of specimen thickness is due to the decrease of plastic zone size near the crack tip and relevant energy change during the crack growth. The effect of specimen thickness on static fatigue lifetime is much greater for cemented carbides with larger WC grain size or higher cobalt content, which is attributed to operative toughening mechanisms.

Keywords: *cemented carbides; static fatigue; size effect; microstructure.*

INTRODUCTION

Cemented carbides or hardmetals belong to a range of powder metallurgical liquid-phase sintered composite materials in which hard and brittle carbides of the transition metals are bound together by a soft and ductile metal binder such as cobalt or nickel [1, 2]. They have become acknowledged forefront materials for metal cutting tools, rock bits, structural component, and wear parts since their birth in 1923 [3, 4]. The success of this composite is mainly due to the combination of its high hardness and strength, good fracture toughness and excellent wear resistance [3, 5]. In order to optimize the design and performance of hardmetal tools and components, an extensive and detailed study is conducted with the main goal of characterizing the microstructure and mechanical behavior of cemented carbides.

The fatigue and fracture of cemented carbides have been a research focus in the past three decades [6–8]. Given the brittle carbide phase content up to 70–97 % in cemented carbides [9], researchers have drawn different conclusions about whether cyclic fatigue or static fatigue plays a dominant role in the fatigue damage of these materials. Lueth [10] found that the fatigue fracture surface was the same as these

produced under static loading and both fracture surfaces showed ductile dimple characteristic in cobalt binder phase. Therefore, he argued that static fracture mode was primary in comparison with cyclic failure mode. Furthermore, Fry and Garrett [11] reported the marked influence of mean stress on the fatigue crack growth (FCG) of cemented carbides, which manifested the existence of static fracture mode together with a true fatigue process. Torres and Llanes [12, 13] noticed a much higher dependency of FCG rate on K_{\max} (the maximum stress intensity factor) than on ΔK (the stress intensity factor range). And this implied the relative dominance of static failure modes in the fatigue process of cemented carbides. Meanwhile, as mean binder free path decreased, a transition from metallic-like to ceramic-like FCG behavior was discerned [13]. Although many researchers found static fracture modes in fatigue, few of them studied the static fatigue of cemented carbides.

As cemented carbides with low binder phase contents resemble high strength brittle ceramic materials in mechanical properties and microstructure coupling with apparent defects, they exhibit distinct size effect on fracture strength like ceramics [14]. Currently the size of cemented carbide tools such as printed circuit board drills, metal cutting tools and cold forging die range from micrometers to meters. The objective of the present work is to shed light on static fatigue mechanism of straight cemented carbides, which will offer a possible method for the evaluation of mechanical properties. At the same time, the influence of specimen thickness on the static fatigue lifetime is investigated when the specimen thickness changes within a narrow range. From the engineering application perspective, the information gathered here gives a theoretical guide for designing and manufacturing cutting tools and drills of cemented carbides.

MATERIALS AND EXPERIMENTAL ASPECTS

In this work, the experiment materials were straight cemented carbides produced by ZhuZhou Cemented Carbide Group Co., LTD. Two series of WC-Co cemented carbides corresponding to four grades with different combinations of carbide grain size and cobalt mass fraction were investigated. Table 1 shows the designations, chemical compositions and key microstructural parameters of each grade. Binder content value was provided by the material manufacturer. Mean carbide grain size was determined by the linear intercept method using scanning electron microscopy images. Whereas binder mean free path thickness (λ_{Co}) and carbide contiguity (C_{WC}) were calculated in accordance with the best-fit equations in the literature [17, 18].

Table 1. Nomenclature and microstructural data for the studied cemented carbides

Grade	Co, wt %	d_{WC} , μm	C_{WC}	λ_{Co} , μm
8EF	8	0.72	0.52	0.22
8F	8	0.95	0.48	0.29
10C	10	3.16	0.35	0.87
15C	15	3.21	0.22	1.22

Conventional mechanical properties of cemented carbides including hardness (HV_{30}), transverse rupture strength (σ_{bb}) and fracture toughness (K_{Ic}) were measured. Hardness testing was carried out on a hardness tester with a Vickers diamond pyramidal indenter applying a load of 294 N. Fracture toughness was evaluated

using 100×20×10 mm single edge notched beam specimens with the notch length-to-width ratio of 0.5. The notch was induced by electrical discharge machining and the notch tip curvature was 20 and 60 μm. A sharp crack was introduced under the compressive cyclic loads and more details can be found in the ASTM E399 standard. Transverse rupture strength test was carried out on rectangular bars of dimensions 45×5×5 mm. The edges of these samples were slightly chamfered in order to avoid stress concentration. For each grade, transverse rupture strength was got from the mean value of sixteen experiments. These were performed on a servo-hydraulic testing machine with a loading rate of 90 N/s. And the results were analyzed by the Weibull statistics.

Static fatigue testing was performed on a servo-hydraulic testing machine under three-point bend loading with a span of 30 mm for the sake of establishing modified stress–failure time diagrams. The test piece dimensions were also 45×5×5 mm, respectively, in L (length of specimen), b (width of test piece perpendicular to its thickness) and h (thickness of test piece parallel to the direction of application of the test force). And the surface of all specimens was polished to mirror-like finish with emery papers and diamond paste before test. Four different stresses were used under the load control, namely 0.95, 0.9, 0.85 and 0.8 times σ_{bb} . At least six specimens were employed for each stress. A time to failure was measured on the flexure specimen subjected to a specified level of stress and this procedure was repeated until all the specimens within the experiment matrix were tested. The tests were stopped if the test piece had not ruptured by 150 hours. In order to investigate the effect of specimen thickness on static fatigue lifetime, a series of specimens with constant width ($b = 5\text{ mm}$) and various thickness ($h = 4.6\text{ mm}, 4.7\text{ mm}, 4.8\text{ mm}, 4.9\text{ mm}$ and 5.0 mm) was prepared. Every specimen with a specific thickness was loaded by identical stress, σ_{bb} of 80 %, to give a failure time with a view to setting up the curves of static fatigue lifetime versus specimen thickness. All tests were conducted at ambient temperature in air.

Finally, a detailed fractographic analysis of broken specimens was carried out by scanning electron microscopy (SEM) to characterize and discern static fatigue mechanisms.

RESULTS AND DISCUSSION

Mechanical properties

Mechanical properties of cemented carbides under consideration such as hardness, transverse rupture strength (σ_{bb}) and fracture toughness (K_{Ic}) are summarized in Table 2.

Table 2. Mechanical properties for the investigated hardmetal grades

Grade	HV_{30} , MPa	K_{Ic} , MPa·m ^{1/2}	σ_{bb} , MPa	Weibull modulus
8EF	1570±22	11.4±0.3	3721±92	13
8F	1496±18	12.7±0.3	3285±61	22
10C	1182±25	15.7±0.2	2871±43	34
15C	1027±30	19.5±0.4	3016±54	45

As shown in Fig. 1, with binder mean free path thickness rising, fracture toughness increases but hardness decreases. This is consistent with the results previously reported [19–21]. However, the trend of transverse rupture strength is different from that of fracture toughness. For hardmetals with the same content of

cobalt (8EF and 8F), the smaller grain size of carbide tungsten contributes to higher transverse rupture strength. However, higher transverse rupture strength is possessed by hardmetal with higher cobalt content (15C) under the circumstance of uniform WC grain size. Moreover, hardmetals with higher hardness possess the larger strength scatters, while those with better toughness have higher Weibull modulus value for transverse rupture strength. As is indicated in Fig. 2, the fractographic aspects of broken specimens subjected to monotonic loading exhibited fracture in the metallic binder interdispersed with cleavage and intergranular fracture of the carbides [13, 22, 23].

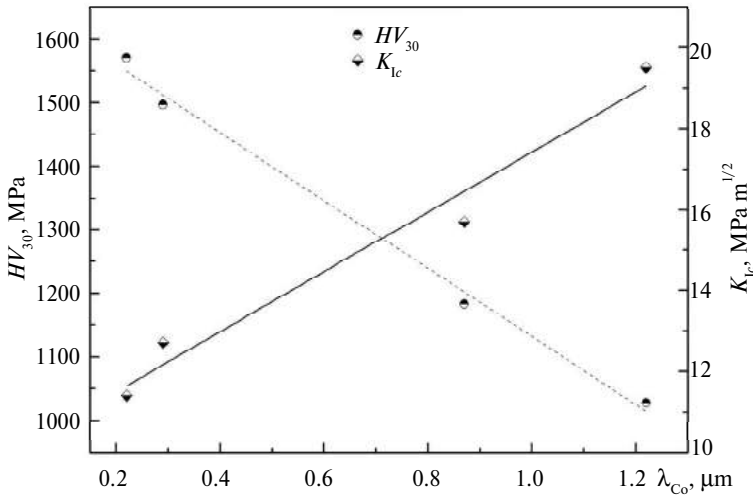


Fig. 1. Plot of experimentally measured hardness and fracture toughness against binder mean free path thickness.

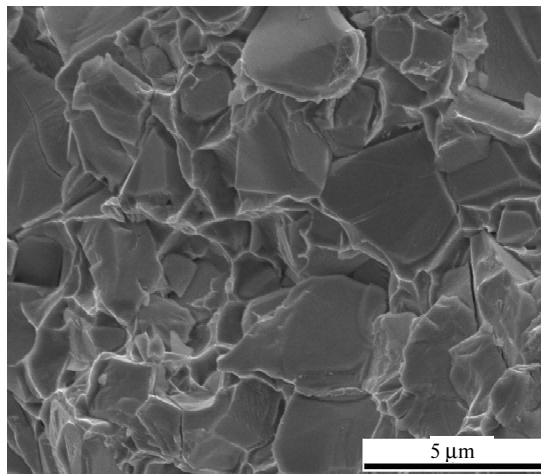


Fig. 2. SEM micrograph showing fractographic aspects of a specimen tested to rupture under monotonic loading.

Fatigue and fracture mechanisms of hardmetals under static loading

As with the brittle ceramic, cemented carbides with low cobalt content display a tendency of subcritical crack growth under static loading [24]. The modified stress-life time curve of three grades is shown in Fig. 3. For this purpose the ratio of the stress to transverse rupture strength (σ/σ_{bb}) is calculated using the applied static

stress (σ) in the static fatigue tests. The experimental results indicate that 8F hardmetal under the stress in excess of 80 % σ_{bb} exhibits time-dependent fracture characteristic. The static fatigue lifetime of 8F hardmetal rises with the decrease of applied static stress. These results are opposite to the Schleinkofer's conclusion that no failure of cemented carbides occurred for 4 months under the static stress less than 95 % σ_{bb} [25, 26].

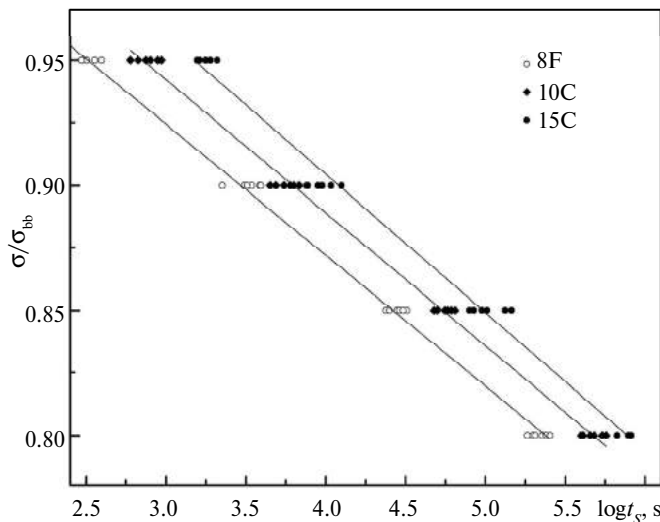


Fig. 3. The relationship between σ/σ_{bb} and static fatigue lifetime for 8F grade.

Cemented carbides are a kind of typical powder metallurgical composites. In the process of powder preparation, pressing and sintering, many intrinsic defects which go against mechanical properties are generated. As shown in Fig. 4, static fatigue fracture surfaces of hardmetals exhibit surface or subsurface processing heterogeneities such as pores, inclusions (Fig. 4, *a*), abnormally large carbides (Fig. 4, *b*), binderless carbide clusters (Fig. 4, *c*), microcracks (Fig. 4, *d*) and cobalt pool [14, 16]. These powder metallurgical defects destroy the continuity of microstructure, which have a negative impact on the load transfer.

When the specimen of 8F hardmetal is subjected to three-point bending load, the defects on the tensile surface and compressive surface, especially pores, microcracks and abnormally large carbides, lead to a great stress concentration near the imperfections. According to theoretical models proposed by Seung et al. [27], the maximum stress near the circular pores on the surface or subsurface of specimens is 2.8 to 4 times higher than the external applied stress during the 3-point bending test. Moreover, the degree of stress concentration is concerned with the size, location and geometry of microstructure defects. The more out-of-shape and larger defects on the surface lead to a greater stress concentration. Therefore, the crack is initiated from pores and large carbides due to the strong stress concentration when the external static stress is applied to the cemented carbides specimens. Once the crack is generated, the degree of stress concentration becomes much stronger, which promotes rapid crack propagation. When the crack encounters other cracks and pores in the crack growth direction, they would connect with each other to form a main crack (Fig. 5) [28].

Furthermore, the formation of main crack may also result from the connection of microcracks and pores which have existed in the material before applying load.

Then the main crack quickly grows up and propagates unstably, resulting in the failure of the specimen under the static stress [29]. The fracture surfaces of the specimens show a typical dimple structure in the binder phase and cleavage fracture through the carbides (Fig. 6) [30]. It is similar to the fracture surface characteristics of failure specimens in the flexure strength tests (see Fig. 2).

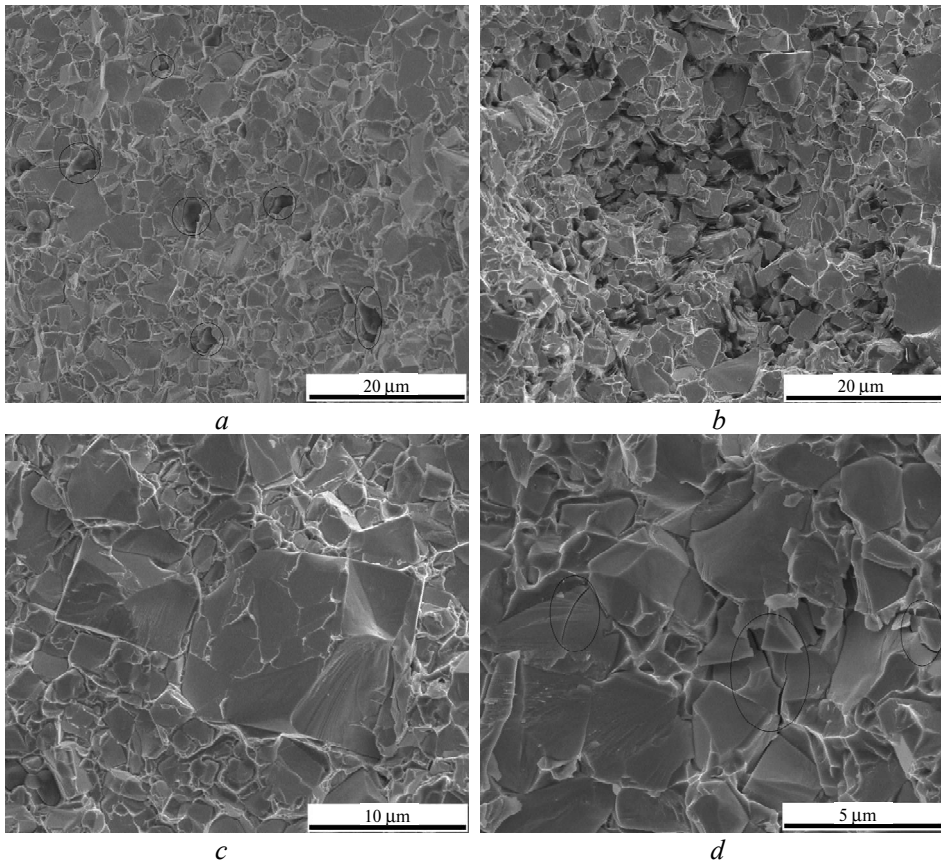


Fig. 4. SEM micrograph of defects as crack initiation site in specimens tested to failure under static fatigue loading: inclusion (a), abnormally large carbides (b), binderless carbide clusters (c), micro cracks (d).

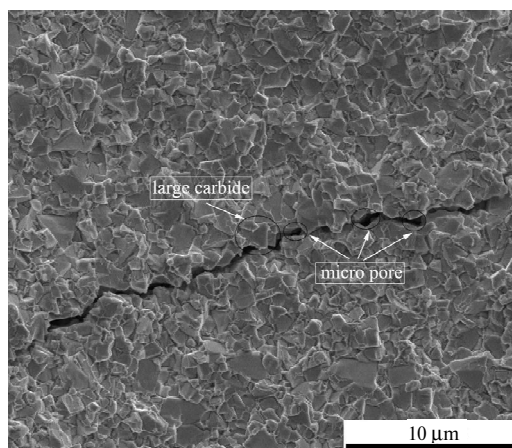


Fig. 5. SEM micrograph of a main crack resulted from the connection of cracks and pores in the crack growth direction.

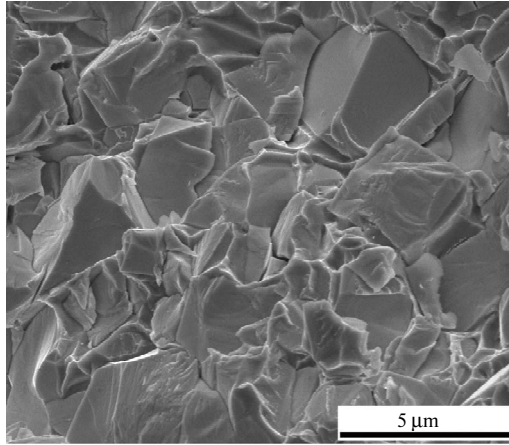


Fig. 6. SEM image showing fractographic feature corresponding to static fatigue loading in the hardmetal studied.

Specimen thickness effects on the static fatigue lifetime of hardmetals

Figure 7 shows the relationship between the static fatigue lifetime (t_s) and specimen thickness (h) for two series of cemented carbides corresponding to four grades under the stress equal to 80 % of respective transverse rupture strength. The each data point in the diagrams is the average values of t_s for eight specimens tested to failure. It can be seen from Fig. 7 that specimen thickness in the present range has an apparent influence on the static fatigue lifetime for cemented carbides with low cobalt content. There is a clear extension of static fatigue lifetime when the specimen thickness increases.

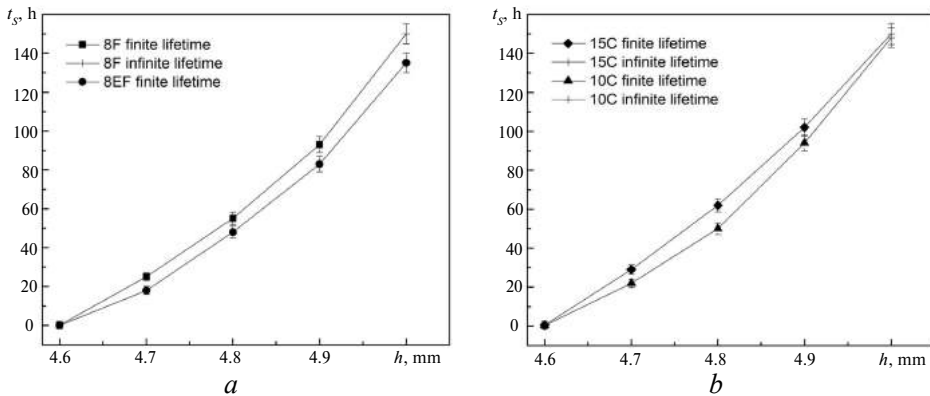


Fig. 7. Effect of specimen thickness on the static fatigue lifetime (t_s) for different hardmetal grades under the stress equal to 80 % of respective transverse rupture strength: 8EF and 8F (a), and 10C and 15C (b).

Few investigations have been carried out about the influence of specimen size on the static fatigue lifetime so far. Torres et al. [14] concluded that the failure probability of large specimens were greater than that of small specimens. Nonetheless, the experiment in this paper confirms that the thicker specimen has longer static fatigue lifetime. This can be explained in terms of the static fatigue crack initiation and propagation.

As is stated above, crack initiation starts from the defects on the surface and subsurface rather than in the interior of cemented carbide specimens bearing static loads. When the thickness of specimen increases from 4.6 mm to 5.0 mm, there is only a slight increase in the specimen volume, but the area of tensile and compressive surface does not change. Based on the above analysis, the increase of specimen thickness has no influence on the number of defects on the surface and subsurface of specimen from the perspective of probability. In other words, the number of crack initiation site keeps constant. Therefore, the static fatigue life at least doesn't decrease when the specimen thickness rises under the same static load.

It is well acknowledged that linear elastic fracture mechanics (LEFM) is an effective approach for analyzing the fracture behavior of cemented carbides, especially the crack propagation. LEFM contains elastic energy theory and stress intensity theory [31]. The following discussions are based on the two theories within the LEFM frame.

According to the Griffith-Irwin fracture theory [31–33], the external load applied to the material is translated to the internal elastic strain energy. In the process of crack growth, the surface energy increases with the occurrence of new crack surface and the fracture of ductile phase is accompanied with the generation of plastic deformation energy. Both plastic deformation energy and newly created surface energy are provided by the elastic strain energy [34]. Thus the condition for the growth of Griffith cracks is as follows:

$$\frac{F^2 L^3}{8Ebh^3} \geq (\gamma_s + \gamma_p) S_{mf}, \quad (1)$$

where F is the applied static load; E is the Young's modulus; γ_s is a specific surface energy and γ_p is specific plastic deformation energy; S_{mf} is the total macroscopic area of fracture surface. The left part of the equation is the elastic strain energy acting as a driving force of the crack growth. The right part is surface energy and plastic deformation energy, serving as the crack growth resistance. When the specimen thickness increases, the elastic strain energy decreases. Meanwhile, surface energy and plastic deformation energy increase due to the rise of a total macroscopic area of the fracture surface. In other words, the driving force of the crack growth decreases and the crack growth resistance increases. Thereby, static crack growth rate slows down with the increase of specimen thickness under the same static stress, and then the static fatigue lifetime is prolonged. The second forceful evidence is involved with the stress intensity theory [31]. Because the width is larger than $2.5(K_{Ic}/\sigma_y)^2$ for all the cemented carbide specimens, the stress state near the crack tip for all the specimens in the static fatigue tests is a plain stress. When the specimen thickness rises, plastic zone size near the crack tip becomes smaller and then static fatigue crack rate decreases [35–38]. Finally, the static fatigue life is naturally extended.

In addition, the influence of specimen thickness on static fatigue lifetime is also affected by the microstructure of cemented carbides. As for cemented carbides with the same content of cobalt, the effect of specimen thickness on static fatigue lifetime is greater when the WC grain size is larger (see Fig. 7, *a*). The same phenomenon occurs if the binder content increases while WC grain size keeps constant (see Fig. 7, *b*). The above results can be rationalized through analyzing the operative toughening mechanisms. On the one hand, microstructural coarsening makes crack deflection become an operative toughening mechanisms and gives rise to a higher transgranular carbide area fraction within crack paths [6, 12]. On the other

hand, cemented carbides with high cobalt content possess more remarkable crack tip shielding effect because of the ductile Co ligament bridging in crack wake [39, 40]. All these make more energy consumed in the process of crack growth. Therefore, the larger the WC grain size or the higher the cobalt content of cemented carbides, the greater the effect of specimen thickness on static fatigue lifetime. Besides, the results shown in Fig. 7 also prove that there is no direct connection between static fatigue and transverse rupture strength.

CONCLUSIONS

The static fatigue fracture mechanism and the effect of specimen thickness on the static fatigue lifetime were investigated on four microstructurally different WC–CO cemented carbides using three-point bending methods. The crack in cemented carbides under static fatigue loads is initiated from surface or subsurface defects such as micropores, abnormally large carbides and binderless carbide clusters. The connection of previous cracks creates the main crack. The subcritical growth of main crack leads to the static fatigue fracture of cemented carbides. The rise of specimen thickness prolongs static fatigue lifetime of cemented carbides subjected to the stress equal to 80 % of respective transverse rupture strength because of relative constant defect number, smaller plastic zone size, the decrease of the elastic strain energy as well as the increase of the surface energy and plastic deformation energy. Larger WC grain size or higher cobalt content creates the greater effect of specimen thickness on static fatigue lifetime.

ACKNOWLEDGMENTS

The authors greatly acknowledge the financial support by open fund of state key laboratory of cemented carbide (201403001).

Досліджено механізм статичної втоми і вплив товщини зразка на термін служби при статичній втомі для чотирьох твердих сплавів WC–Co з різним вмістом зв'язки і розміром зерен. Випробування на статичну втому при навантаженні за схемою триточкового вигину було проведено на зразках різних розмірів. Поверхні зламів зруйнованих зразків було вивчено з допомогою скануючої електронної мікроскопії з метою дослідження мікромеханізму статичної втоми. Експериментальні результати показують, що мікротріщини виникають в присутності дефектів або неоднорідностей, а з'єднання мікротріщин створює основну тріщину. Основна тріщина швидко поширюється і в результаті зразки руйнуються. Збільшення періоду стійкості зразків, випробуваних на статичну втому, зі збільшенням товщини зразків викликано зменшенням розміру пластичної зони поблизу вершини тріщини і істотною зміною енергії при зростанні тріщини. Вплив товщини зразка на термін служби при статичній втомі значно більше для твердих сплавів з WC-зернами більшого розміру або при більш високому вмісті кобальту, що пов'язано з діючими механізмами в'язкого руйнування.

Ключові слова: твердий сплав, статична втома, розмірний ефект, мікроструктура.

Исследованы механизм статической усталости и влияние толщины образца на срок службы при статической усталости для четырех твердых сплавов WC–Co с различным содержанием связующего и размером зерен. Испытания на статическую усталость при нагрузке по схеме трехточечного изгиба были проведены на образцах различных размеров. Поверхности изломов разрушенных образцов были изучены с помощью сканирующей электронной микроскопии с целью исследования микромеханизмов статической усталости. Экспериментальные результаты показывают, что микротрещины возникают в присутствии дефектов или неоднородностей, а соединение микротрещин создает основную трещину. Основная трещина быстро распространяется и в результате образцы разрушаются. Увеличение периода стойкости образцов, испытанных на статическую усталость, с увеличением толщины образцов вызвано уменьшением

размера пластической зоны вблизи вершины трещины и существенным изменением энергии при росте трещины. Влияние толщины образца на срок службы при статической усталости значительно больше для твердых сплавов с WC-зернами большего размера или при более высоком содержании кобальта, что связано с действующими механизмами вязкого разрушения.

Ключевые слова: твердый сплав, статическая усталость, размерный эффект, микроструктура.

1. Upadhyaya G. S. Materials science of cemented carbides – An overview // Mater. Des. – 2001. – 22, N 6. – P. 483–489.
2. Exner H. E. Physical and chemical nature of cemented carbides // Int. Met. Rev. – 1979. – 24, N 1. – P. 149–173.
3. Sarin V. K., Mari D., Llanes L. Comprehensive Hard Materials. Vol. 1: Hardmetals. – UK: Elsevier, 2014.
4. Voort, G.F.V., Metallography and Microstructure, vol. 9 of ASTM Handbook, USA: ASM International, 2004.
5. Raihanuzzaman R. M., Xie Z., Hong S. J., Ghomashchi R. Powder refinement, consolidation and mechanical properties of cemented carbides – An overview // Powder Technol. – 2014. – 261. – P. 1–13.
6. Torres Y., Tarrago J. M., Coureaux D., Tarrés E., Roebuck B., Chan P., James M., Liang B., Tillman M., Viswanadham R. K., Mingard K. P., Mestra A., Llanes L. Fracture and fatigue of rock bit cemented carbides: Mechanics and mechanisms of crack growth resistance under monotonic and cyclic loading // Int. J. Refract. Met. Hard Mater. – 2014. – 45. – P. 179–188.
7. Mikado H., Ishihara S., Oguma N., Masuda K., Kitagawa S., Kawamura S. Effect of stress ratio on fatigue lifetime and crack growth behavior of WC–Co cemented carbide // Trans. Nonferrous Met. Soc. – 2014. – 24. – P. 14–19.
8. Tarragó J.M., Jiménez-Piqué E., Turón M., Rivero L., Schneider L., Llanes L. Toughening and fatigue micromechanisms in hardmetals: FESEM/FIB Tomography Characterization // Proc. 18th Plansee Seminar, Reutte/Tyrol, Austria, 3–7 June, 2013. – Vol. 54. – P. 1–9.
9. Laperrière L., Reinhart G. CIRP Encyclopedia of Production Engineering, Berlin Heidelberg: Springer, 2014
10. Lueth R. C. Fatigue of WC–Co cemented carbide // J. Eng. Mater. Technol. – 1981. – 103. – p. 180–185.
11. Fry P. R., Garrett G. G. Fatigue crack growth behavior of tungsten carbide–cobalt hardmetals // J. Mater. Sci. – 1988. – 23, N 7. – P. 2325–2338.
12. Llanes L., Torres Y., Anglada M. On the fatigue crack growth behavior of WC–Co cemented carbides: kinetics description, microstructural effects and fatigue sensitivity // Acta Mater. – 2002. – 50, N 9. – P. 2381–2393.
13. Torres Y., Anglada M., Llanes L. Fatigue mechanics of WC–Co cemented carbides // Int. J. Refract. Met. Hard Mater. – 2001. – 19. – P. 341–348.
14. Torres Y., Bermejo R., Gotor F. J., Chicardi E., Llanes L. Analysis on the mechanical strength of WC–Co cemented carbides under uniaxial and biaxial bending // Mater. Des. – 2014. – 55. – P. 851–856.
15. Weibull W. A statistical representation of fatigue failures in solids, Elander, 1949.
16. Klünsner T., Wurster S., Supancic P., Ebner R., Jenko M., Glätzle J., Püschel A., Pippan R. Effect of specimen size on the tensile strength of WC–Co hard metal // Acta Mater. – 2011. – 59, N 10. – P. 4244–252.
17. Tarragó J. M., Coureaux D., Torres Y., Wu F., Al-Dawery I., Llanes L. Implementation of an effective time-saving two-stage methodology for microstructural characterization of cemented carbides, Int. J. Refract // Met. Hard Mater. – 2016. – 55. – P. 80–86.
18. Roebuck B., Almond E. A. Deformation and fracture processes and the physical metallurgy of WC–Co hardmetals // Int. Met. Rev. – 988, vol. 33, no. 1, pp. 90–112.
19. Dias A. M. S., Miranda J. S., Godoy G. C. Evaluation of fracture toughness by indentation testing in hardmetal tools // Materia. – 2009. – 14, N 2. – P. 869–877.
20. Ravichandran K. S. Fracture toughness of two phase WC–Co cermets // Acta Mater. – 1994. – 42, N 1. – P. 143–150.
21. Sigl L. S., Fischmeister H. F. On the fracture toughness of cemented carbides // Acta Metall. – 1988. – 36, N 4. – P. 887–897.

22. Exner H. E., Sigl L., Fripan M., Pompe O. Fractography of critical and subcritical cracks in hard materials // *Int. J. Refract. Met. Hard Mater.* – 2001. – **19**, N 4. – P. 329–334.
23. Erling G., Kursawe S., Luyckx S., Sockel H. G. Stable and unstable fracture surface features in WC–Co // *J. Mater. Sci. Lett.* – 2000. – **19**, N 5. – P. 437–438.
24. Suresh S. *Fatigue of materials.* – UK: Cambridge university press, 1998.
25. Schleinkofer U., Sockel H. G., Görting K., Heinrich W. Fatigue of hard metals and cermets // *Mater. Sci. Eng. A.* – 1996. – **209**, N 1. – P. 313–317.
26. Schleinkofer U., Sockel H. G., Schlund P., Görting K., Heinrich W. Behaviour of hard metals and cermets under cyclic mechanical loads // *Mater. Sci. Eng. A.* – 1995. – **194**, N 1. – P. 1–8.
27. Cha S. I., Lee K. H., Ryu H. J., Hong S. H. Effect of size and location of spherical pores on transverse rupture strength of WC–Co cemented carbides // *Mater. Sci. Eng. A.* – 2008. – **486**, N 1. – P. 404–408.
28. Wilkinson D. S., Vitek V. The propagation of cracks by cavitation: a general theory // *Acta Metall.* – 1982. – **30**, N 9. – P. 1723–1732.
29. Liu W., Chen Z. H., Wang H. P., Zhang Z. J., Yao L., Chen D. Small Energy Multi-Impact and Static Fatigue Properties of Cemented Carbides // *Powder Metall. Met. Ceram.* – 2016. – **55**, N 5. – P. 312–318.
30. Teppernegg T., Klünsner T., Kreamsner C., Tritremmel C., Czettel C., Puchegger S., Marsoner S., Pippan R., Ebner R. High temperature mechanical properties of WC–Co hard metals // *Int. J. Refract. Met. Hard Mater.* – 2016. – **56**. – P. 139–144.
31. Anderson T. L. *Fracture Mechanics: Fundamentals and Applications.* – Raton: CRC Press, 2005.
32. Sanders J. L. On the Griffith–Irwin Fracture Theory // *J. Appl. Mech.* – 1960. – **27**, N 2. – P. 352–355.
33. Griffith A. A. The phenomena of rupture and flow in solids // *Philos. Trans. R. Soc. A.* – 1921. – **221**, N 582. – P. 163–198.
34. Yanaba Y., Hayashi K. Relation between fracture surface area of a flexural strength specimen and fracture toughness for WC–10mass%Co cemented carbide and Si₃N₄ ceramics // *Mater. Sci. Eng. A.* – 1996. – **209**, N1. – P. 169–174.
35. Banerjee S. Influence of specimen size and configuration on the plastic zone size, toughness and crack growth // *Eng. Fract. Mech.* – 1981. – **15**, N 3. – P. 343–390.
36. Putatunda S. K., Banerjee S. Effect of size on plasticity and fracture toughness // *Eng. Fract. Mech.* – 1984. – **19**, N 3. – P. 507–529.
37. Rosenberg, G., The size of plastic zones and fatigue crack growth behavior of three forms of a Ti–6Al–2.5Mo–1.5Cr alloy // *Fatigue Fract. Eng. Mater. Struct.* – 1998. – **21**, N 6. – P. 727–739.
38. Korda A. A., Miyashita Y., Mutoh Y. The role of cyclic plastic zone size on fatigue crack growth behavior in high strength steels // *The 5th Int. Conf. on Mathematics and Natural Sciences, Timisoara, Romania, 2–4 June, 2004.* – Timisoara, the West University of Timisoara, 2004. – Vol. 1677. – P. 070013.
39. Tarrago J. M., Jimenez-Pique E., Schneider L., Casellas D., Torres Y., Llanes L. FIB/FESEM experimental and analytical assessment of R-curve behavior of WC–Co cemented carbides // *Mater. Sci. Eng. A.* – 2015. – **645**. – P. 142–149.
40. Tarragó J. M., Coureaux D., Torres Y., Casellas D., Al-Dawery I., Schneider L., Llanes L. Microstructural effects on the R-curve behavior of WC–Co cemented carbides // *Mater. Des.* – 2016. – **97**. – P. 492–501.

Received 26.12.16